CellPress
PARTNER JOURNAL

SNOWY COTYLEDON 2 Promotes Chloroplast Development and Has a Role in Leaf Variegation in Both *Lotus japonicus* and *Arabidopsis thaliana*

Nicola Zagari[1,2,3], Omar Sandoval-Ibañez[2], Niels Sandal[4], Junyi Su[4],
Manuel Rodriguez-Concepcion[5], Jens Stougaard[4], Mathias Pribil[2], Dario Leister[1,2,*]
and Pablo Pulido[1,2]

[1]Plant Molecular Biology, Department of Biology I, Ludwig-Maximilians-Universität München, 82152 Planegg-Martinsried, Germany

[2]Copenhagen Plant Science Center, University of Copenhagen, 1871 Frederiksberg C, Denmark

[3]Research and Innovation Center, Fondazione Edmund Mach, via E. Mach 1, 38010 San Michele all'Adige, Italy

[4]Centre for Carbohydrate Recognition and Signalling, Department of Molecular Biology and Genetics, Aarhus University, Gustav Wieds Vej 10, 8000 Aarhus C, Denmark

[5]Centre for Research in Agricultural Genomics (CRAG) CSIC-IRTA-UAB-UB, Campus UAB Bellaterra, 08193 Barcelona, Spain

*Correspondence: Dario Leister (leister@lmu.de)

ABSTRACT

Plants contain various factors that transiently interact with subunits or intermediates of the thylakoid multi-protein complexes, promoting their stable association and integration. Hence, assembly factors are essential for chloroplast development and the transition from heterotrophic to phototrophic growth. Snowy cotyledon 2 (SCO2) is a DNAJ-like protein involved in thylakoid membrane biogenesis and interacts with the light-harvesting chlorophyll-binding protein LHCB1. In *Arabidopsis thaliana*, SCO2 function was previously reported to be restricted to cotyledons. Here we show that disruption of *SCO2* in *Lotus japonicus* results not only in paler cotyledons but also in variegated true leaves. Furthermore, smaller and pale-green true leaves can also be observed in *A. thaliana sco2* (*atsco2*) mutants under short-day conditions. In both species, SCO2 is required for proper accumulation of PSII–LHCII complexes. In contrast to other variegated mutants, inhibition of chloroplastic translation strongly affects *L. japonicus sco2* mutant development and fails to suppress their variegated phenotype. Moreover, inactivation of the suppressor of variegation AtClpR1 in the *atsco2* background results in an additive double-mutant phenotype with variegated true leaves. Taken together, our results indicate that SCO2 plays a distinct role in PSII assembly or repair and constitutes a novel factor involved in leaf variegation.
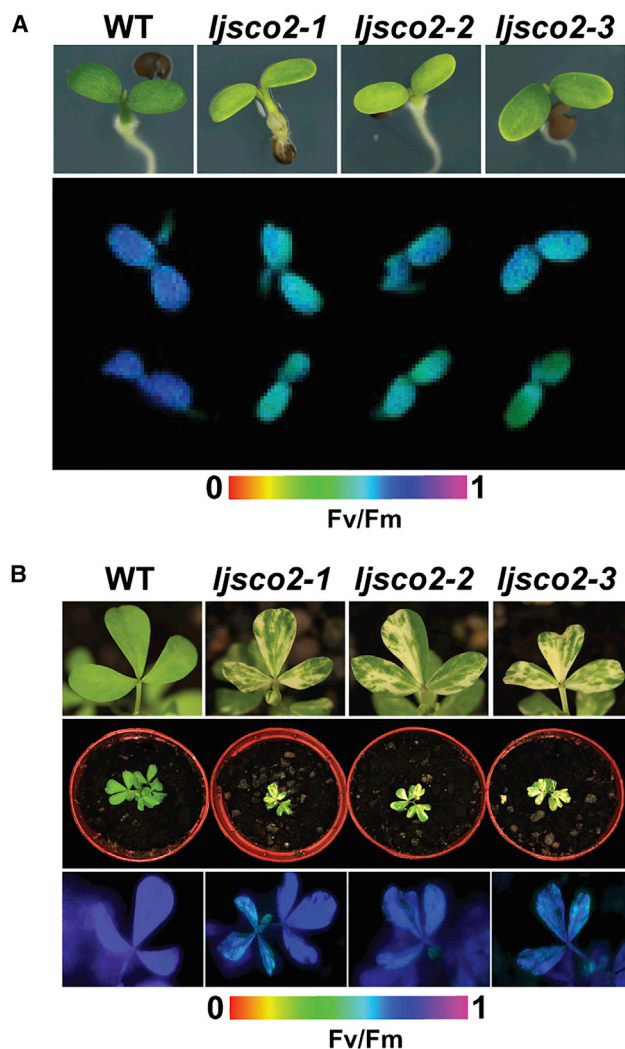
Key words: SCO2, DNAJ-like, photosynthesis, assembly factor, variegation, chloroplast development

INTRODUCTION

According to the endosymbiotic theory, plastids are derived from an engulfed photosynthetic cyanobacterium. The term "plastid" itself refers to the plasticity of this organelle and, indeed, plants contain many different types of plastids, such as leucoplasts, amyloplasts, chromoplasts, and chloroplasts, all of which originate from small, undifferentiated "proplastids" (Lopez-Juez and Pyke, 2005; Sakamoto et al., 2008). During the transition from proplastid to chloroplast (chloroplast biogenesis) a large increase in size is accompanied by the accumulation of pigments (carotenoids and chlorophylls), biosynthesis of

the photosynthetic proteins, and formation of the thylakoid membrane. The final steps, involving the assembly of the light-harvesting antenna complexes (LHCs), are also important for the operation of photosynthesis in the fully developed organelle (Jarvis and Lopez-Juez, 2013). During evolution, plastid genes have been largely transferred to the nucleus, and constant exchange of information between nucleus and chloroplast is necessary to coordinate the production of the photosynthetic

---

Figure 1. Mutation in *LjSCO2* Impairs Chloroplast Development in Cotyledons and True Leaves in *Lotus japonicus*.
Representative pictures of 4-day-old cotyledons **(A)** and 3-week-old **(B)** *Lotus* wild-type (WT) plants and *ljsco2* mutants are shown (upper panels). The photosynthetic parameter F_v/F_m (maximum quantum yield of PSII) was measured using an Imaging PAM system as described in Methods (lower panels). Signal intensities for F_v/F_m are indicated in accordance with the color scale (bar at bottom).

components encoded in each compartment (Ruckle and Larkin, 2009; Kleine and Leister, 2016).

In *Arabidopsis thaliana*, many mutants in which chloroplast biogenesis is compromised exhibit a pale or albino phenotype. A few of these mutants have variegated leaves, made up of groups of cells in which chloroplast development has proceeded normally, while being impaired in others. The current view is that this reflects the existence of a "molecular threshold," below which chloroplast biogenesis comes to a premature halt, producing white sectors (Aluru et al., 2006; Putarjunan et al., 2013). Usually, variegation affects only true leaves, while cotyledons are green because they act as storage organs during heterotrophic growth. In fact, cotyledons are formed during embryogenesis and are developmentally distinct from true leaves (Stoynova-
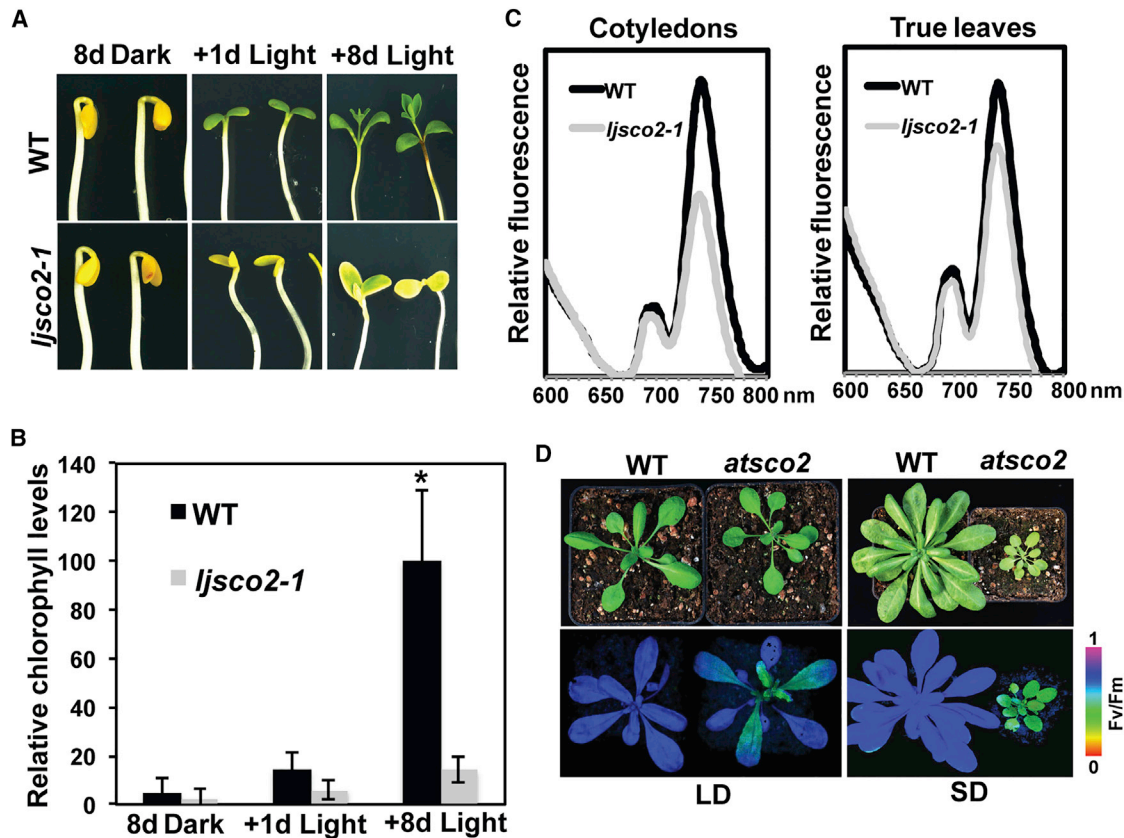
Bakalova et al., 2004). However, one class of *A. thaliana* mutants, the "snowy cotyledon" mutants, display pale/albino cotyledons and green true leaves (Albrecht et al., 2006, 2008, 2010). The gene *SNOWY COTYLEDON 2* (*SCO2*)/CYO1 encodes a DNAJ-like protein with a conserved zinc-finger domain, and is required for normal accumulation of the photosynthetic machinery in cotyledons (Shimada et al., 2007; Albrecht et al., 2008). Other chloroplastic members of the DNAJ-like family have been shown to exhibit chaperone/assembly activity. For instance, PSA2 is required for proper photosystem I (PSI) assembly (Fristedt et al., 2014), LQY1 for photosystem II (PSII) repair after stress (Lu et al., 2011), and OR for accumulation of its substrate phytoene synthase in carotenoid biosynthesis (Zhou et al., 2015). Similarly, SCO2/CYO1 is required for the accumulation of the light-harvesting chlorophyll-binding protein LHCB1 (Tanz et al., 2012). However, it has been proposed to facilitate targeting of LHCB1 to the thylakoid membrane rather than having a function in the assembly of the photosynthetic complexes (Tanz et al., 2012). In addition, SCO2/CYO1 was found to interact with several PSI and PSII subunits in yeast two-hybrid experiments (Muranaka et al., 2012).

In this work, we report that mutations in *SCO2* are associated with leaf variegation in *Lotus japonicus*, and that development of true leaves is also affected in the *A. thaliana sco2* mutant (*atsco2*) under short-day conditions. In both plant species, we demonstrate a role for SCO2 in the assembly or repair of photosystem complexes. Furthermore, an *A. thaliana* double mutant in which *atsco2* is combined with a mutation in *SUPPRESSOR OF VARIEGATION2* (*svr2/atclpr1*) shows an unexpected additive variegated phenotype. Therefore, we propose a mechanistic model for SCO2-dependent variegation, which is insensitive to previously described suppressors of variegation.

RESULTS

Disruption of *SCO2* Results in Leaf Variegation and Stunted Growth in *L. japonicus*

L. japonicus is a model legume for which mutant lines based on the endogenous retrotransposon *LORE1* have been made publicly available (Fukai et al., 2012; Urbanski et al., 2012). New mutants were recently released, some of which display albino or variegated phenotypes (Malolepszy et al., 2016). In this work we identified three different mutant lines, *ljsco2-1* (30096086), *ljsco2-2* (30099994), and *ljsco2-3* (30006602), in which the coding region of the *SCO2* gene (*LjSCO2*; *Lj3g3v0537380*) is disrupted (Supplemental Figure 1). The open reading frame of *LjSCO2* consists of three exons, coding for a protein of 190 amino acids. In *A. thaliana*, loss of *SCO2* (*AtSCO2*) function results in pale/albino cotyledons but normal true leaves (Shimada et al., 2007; Albrecht et al., 2008). Similarly, *ljsco2* mutants displayed paler cotyledons with lower maximum quantum yield (F_v/F_m), indicating functional impairment of PSII (Figure 1A). However, the defects in chloroplast development in *ljsco2* mutants also extended to true leaves, which exhibit a variegated phenotype and lower maximum F_v/F_m of PSII in the white areas (Figure 1B). Among 48 *ljsco2-1* and 70 *ljsco2-2* plants obtained by selfing of plants hemizygous for the respective *LORE1* insertion in the *LjSCO2* gene, we identified 15 and 17 variegated plants,

Figure 2. Greening and Photosynthetic Measures Confirm Conserved Roles of SCO2 between *A. thaliana* and *L. japonicus*.
(A) In the greening experiments, *Lotus* wild-type (WT) and *ljsco2-1* were grown in darkness for 8 days and then exposed to light for one or 8 days.
(B) Quantification of total chlorophyll accumulation during the greening experiments was carried out as described in Methods. Data correspond to the mean and SD values of three independent experiments and are expressed as relative levels (WT plants after 8 days of light = 100%). Statistically significant differences relative to WT in darkness are indicated (*$P < 0.05$, *t*-test).
(C) The 77-K fluorescence emission spectrum was analyzed for *Lotus* cotyledons and true leaves. The fluorescence emission signals were normalized to the minimum at 670 nm. Representative experiments are shown for the WT (black lines) and the *ljsco2-1* mutant (gray lines).
(D) Phenotype of 24-day-old (long-day, LD) and 8-week-old (short-day, SD) *Arabidopsis* WT and the *atsco2* mutant. Signal intensities for F_v/F_m are indicated in accordance with the color scale (right bar).

respectively, which were all homozygous for the *LORE1* insertion, demonstrating perfect linkage between disruption of the *LjSCO2* gene and the leaf phenotype. All three mutants are knockouts for the *LjSCO2* gene (Supplemental Figure 1B). Unfortunately, the antibody raised against AtSCO2 was not able to detect the *Lotus* isoform in Western blot assays. The expression level of *LjSCO2* is higher in cotyledons compared with true leaves, similar to as described in *Arabidopsis*, with higher transcript and protein levels in 5-day-old seedlings compared with rosette or cauline leaves (Shimada et al., 2007). The *ljsco2* mutants are also characterized by stunted root and shoot growth (Supplemental Figure 1D) and reduced size (Supplemental Figure 1E), in which variegation in leaves is independent of developmental stage. These results indicate that SCO2 is involved in suppressing leaf variegation in *Lotus*.

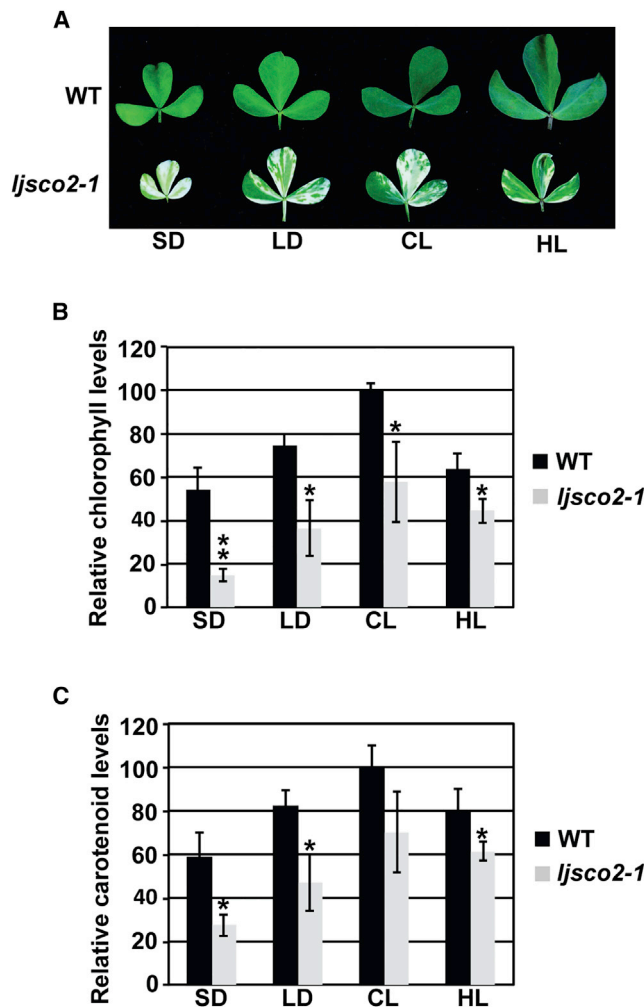### AtSCO2 Orthologs Are Highly Conserved and Belong to the Same Phylogenetic Clade

The different phenotypes observed in *Arabidopsis* and *Lotus sco2* mutants raised the question of whether the function of the protein is conserved. An alignment with orthologous protein sequences

from various plant species revealed that, in all species investigated, SCO2 has a C-terminal DNAJ-like zinc-finger domain, which contains two pairs of cysteines (CXXC) and three additional, highly conserved Cys residues (Supplemental Figure 2A). These cysteines have been proposed to play an important role in the interaction with AtSCO2 substrates (Muranaka et al., 2012). Interestingly, one of the additional cysteines is replaced by its close structural analog serine in the *Lotus* isoform. Phylogenetic analysis of AtSCO2 orthologs and other reported DNAJ-like proteins from *Arabidopsis* demonstrated that all SCO2 proteins belong to the same clade (Supplemental Figure 2B). These results suggest that SCO2 from *Arabidopsis* and *Lotus* may be true functional orthologs.

SCO2 Function Is Conserved between *A. thaliana* and *L. japonicus*

To test whether the SCO2 function is indeed conserved in *L. japonicus*, we performed greening experiments. Seedlings kept in darkness for 8 days were exposed to light for 1 or 8 days (Figure 2A). Like the *Arabidopsis* mutant (Albrecht et al., 2008), plants lacking LjSCO2 failed to accumulate pigments

Figure 3. Analysis of Leaf Phenotype of the *ljsco2-1* Mutant under Different Growth Conditions.

Phenotypes of representative leaf of 45-day-old *Lotus* wild-type (WT) and *ljsco2-1* mutant grown under short-day (SD), long-day (LD), continuous-light (CL), or high-light (HL) conditions **(A)**. Plant material was collected and standard pigment amounts were determined as described in Methods. Relative values of total chlorophyll **(B)** and carotenoids **(C)** are provided (WT grown in CL = 100%). Data correspond to the mean and SD values of n = 4 independent experiments (Student's *t*-test: *$P < 0.05$ and **$P < 0.01$).

upon exposure to light. Quantification of total chlorophyll clearly showed a reduction in chlorophyll accumulation (Figure 2B).

To further investigate photosystem functionality, we carried out measurements of the 77-K fluorescence emission spectra, which allowed us to quantify PSI (peak at 737 nm) and PSII (peak at 693 nm) levels in *Lotus* cotyledons and true leaves. As previously reported for *Arabidopsis* (Albrecht et al., 2008), in the *ljsco2-1* mutant the height of the PSI-specific peak was markedly reduced in both cotyledons and true leaves (Figure 2C). Analysis of isolated chloroplasts using the same amount of chlorophyll confirmed the results obtained directly on true leaves (Supplemental Figure 3).
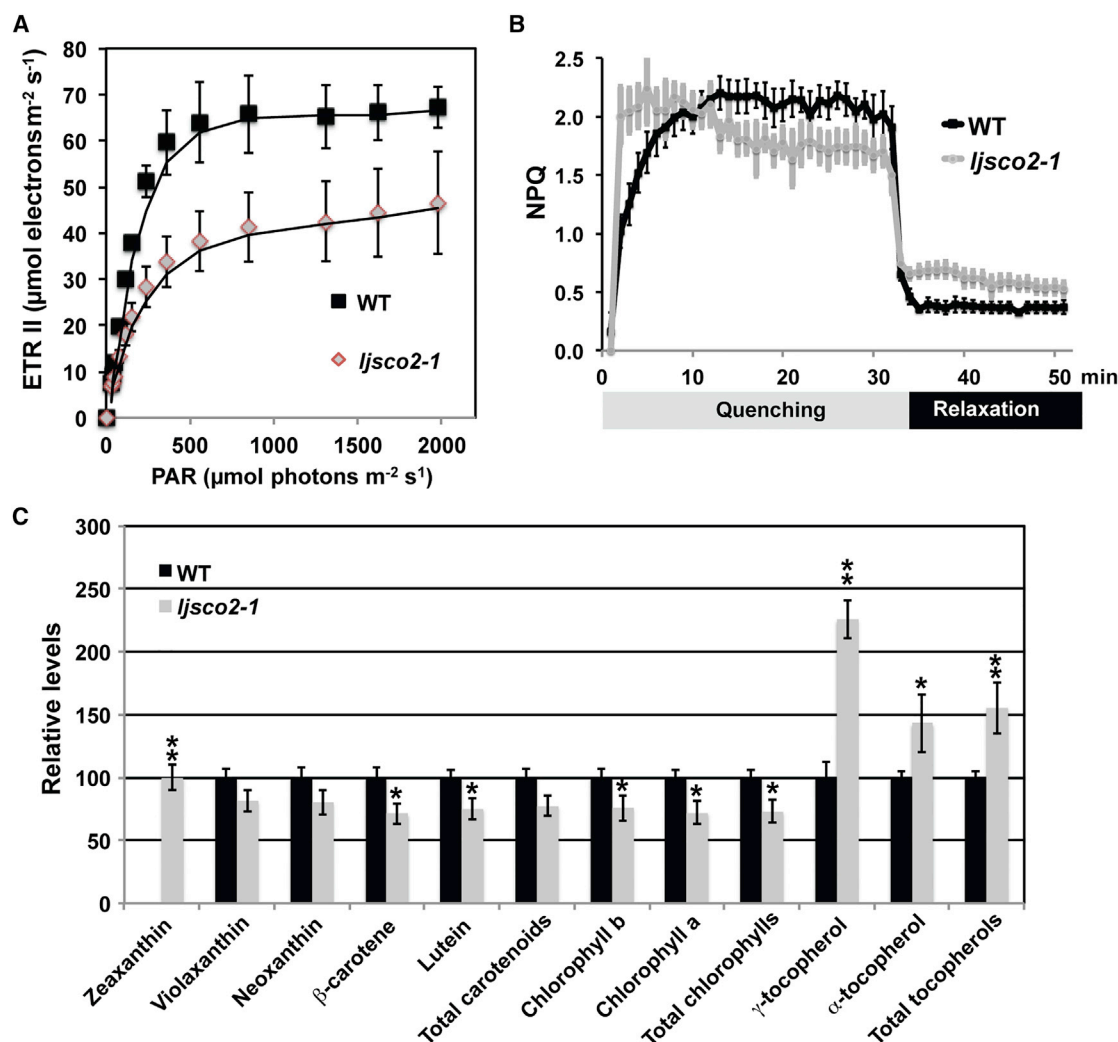
Although variegation in the *Arabidopsis atsco2* mutant has not been observed in photosynthetically competent leaves, we

measured the effects of different light regimes on growth. Strikingly, under short-day conditions *atsco2* plants showed a decrease in growth as well as paler coloration (Figure 2D). F_v/F_m values were lower in true leaves in *atsco2* mutant compared with wild-type (WT) plants, in particular under short-day conditions (Figure 2D). We thus conclude that, as in *ljsco2* plants, cotyledons and true leaves are affected in *atsco2* mutants. Moreover, we found that *atsco2* cotyledons are not only paler in plants grown under short-day conditions, but also under continuous light (Supplemental Figure 4A). Quantification of chlorophylls and carotenoids showed that, in *atsco2* plants, levels of both pigments are higher under the long-day regime, whereas in WT seedlings pigment levels were maximized in continuous light (Supplemental Figure 4B and 4C).

To study the effects of growth conditions and light intensity on leaf variegation of *Lotus* mutants, we grew WT and *ljco2-1* mutant under short-day, long-day, continuous-light, and high-light conditions (see Methods). Similar to the *Arabidopsis* mutant, *ljsco2-1* is paler and smaller under short-day conditions (Figure 3A). Accordingly, quantification of chlorophylls and carotenoids showed that *ljsco2-1* accumulates less than 50% of WT pigment levels (Figure 3B and 3C). Interestingly, although true leaves are variegated in all conditions tested, this phenotype is less pronounced when plants were grown under high light, resulting in lower differences in pigment levels between WT and *ljsco2-1* plants.

LjSCO2 Is Essential for Normal Photosynthetic Performance in *L. japonicus*

Changes in 77-K fluorescence emission demonstrated that PSI is affected in the *ljsco2-1* mutant. Furthermore, measurements of F_v/F_m in plants that had been dark-adapted for 30 min showed that PSII photosynthetic efficiency is also reduced in *ljsco2-1* leaves (0.64 ± 0.07) compared with WT (0.76 ± 0.02), similarly to cotyledons (Figure 1A). Light-response experiments using increasing light intensities confirmed lower electron transport rates for PSII (ETR II) in the *ljsco2-1* mutant compared with WT (Figure 4A). The *ljsco2-1* mutant also differs from the WT with respect to the kinetics of transient NPQ (non-photochemical quenching) induction (Figure 4B). NPQ was analyzed in dark-adapted plants by exposing them to high light levels (830 μmol photons m^{-2} s^{-1}) for 30 min, followed by 15 min of darkness. At the beginning of the light period, NPQ was higher in the *ljsco2-1* mutant than in WT, whereas after 10 min the situation had reversed. In the subsequent dark period (relaxation), values of NPQ dropped in both genotypes, but remained higher in the mutant. The faster NPQ induction in the mutant suggested a pre-accumulation of zeaxanthin in the mutant. Indeed, HPLC experiments confirmed that zeaxanthin highly accumulates in the *ljsco2-1* mutant under low-light conditions, whereas it is only detected in WT plants when grown under high light (Figure 4C and Supplemental Figure 5). Interestingly, tocopherols were also present at higher levels in the mutant, suggesting a constitutive upregulation of antioxidant metabolism. NPQ includes several components, one of which may involve LHC antenna proteins (Niyogi and Truong, 2013). Because SCO2 interacts with LHCB1 (Tanz et al., 2012), it was not surprising to find that absence of SCO2 can affect NPQ formation. However, while antisense lines for LHCB1 are compromised in NPQ, the kinetics of NPQ has

Figure 4. *L. japonicus ljsco2-1* Mutant Displays Impaired Photosynthesis.

Chlorophyll fluorescence parameters of 6-week-old *Lotus* WT and *ljsco2-1* mutant grown under long-day conditions were analyzed using a Dual-PAM system as described in Methods.

(A) Electron transport rate of PSII (ETR II) was calculated at different light intensities in light-response curve.

(B) For non-photochemical quenching (NPQ) analysis, plants were kept in the dark overnight prior to measurements. Gray and black bars indicate periods of illumination with actinic light and intervals in the dark, respectively. Data in **(A)** and **(B)** are representative of at least three independent experiments. Means and SD values are for n ≥ 5 different plants.
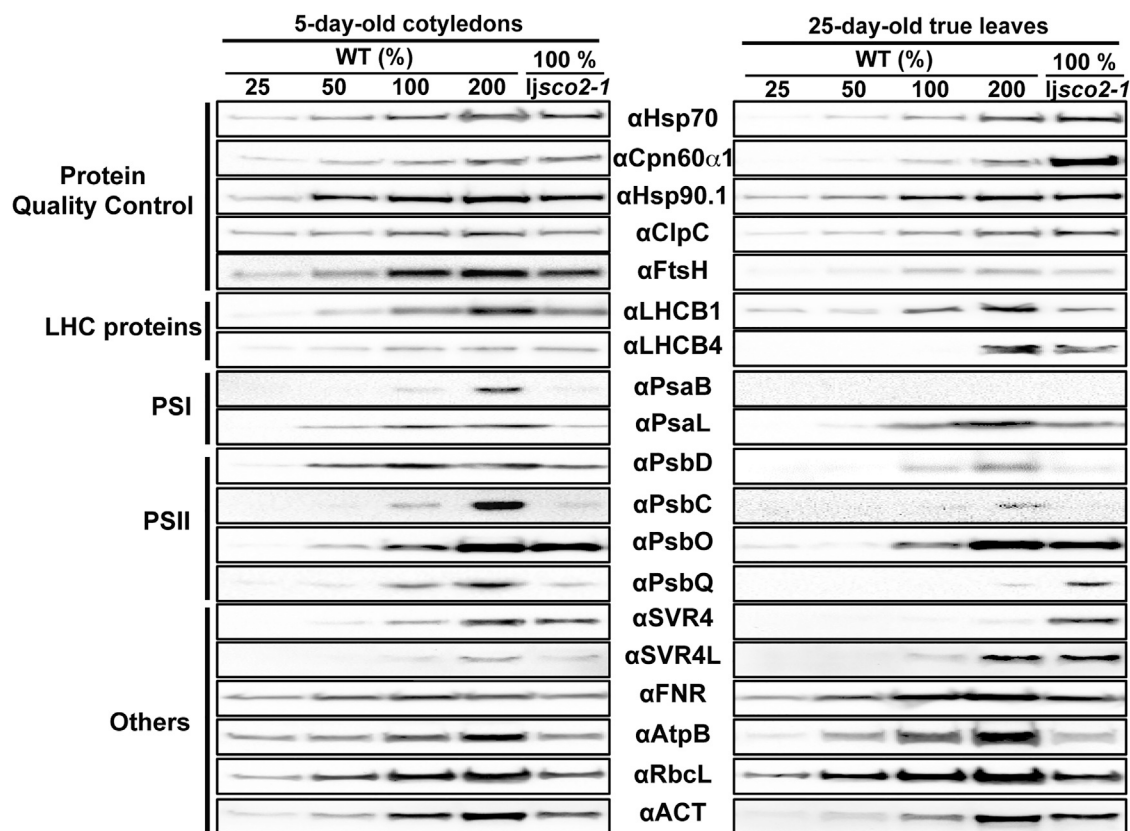
(C) Metabolite analysis by HPLC was performed with the *L. japonicus* plants as described in Methods. Except in the case of zeaxanthin, values relative to the WT plants are provided (absolute values are shown in Supplemental Figure 5). Data correspond to the mean and SD values of n = 4 independent experiments (Student's *t*-test: *$P < 0.05$ and **$P < 0.01$).

been shown to be similar to WT (Pietrzykowska et al., 2014). Therefore, SCO2 might have additional roles in modulating photosynthesis.

Variegated True Leaves Display Markedly Altered Protein Profiles in *L. japonicus*

To compare the effects of mutations in *Lj*SCO2 in cotyledons and variegated true leaves, we analyzed several chloroplastic pathways by immunoblotting using specific antibodies (see Methods). Since SCO2 is a DNAJ-like protein, with potential chaperone/protein disulfide isomerase activity (Shimada et al., 2007; Albrecht et al., 2008; Muranaka et al., 2012), we first looked at components of the protein quality control system, including

chaperones and proteases (Figure 5). Although there is no clear difference between mutant and WT cotyledons, chaperone and protease levels are increased in variegated true leaves in the *ljsco2-1* mutant. These results, together with zeaxanthin and tocopherol accumulation, appear to confirm the upregulation of the antistress machinery in the true leaves in the *ljsco2-1* mutant. Less LHCB1 was detected in the mutant than in the WT (Figure 5), as reported for the *atsco2* mutant of *Arabidopsis* (Shimada et al., 2007; Albrecht et al., 2008; Tanz et al., 2012). The downregulation of LHCB1 was confirmed in the other two *ljsco2* mutants (in contrast to higher levels of Hsp70) (Supplemental Figure 6A). The upregulation of LHCB4 in *ljsco2-1* suggests the activation of compensatory mechanisms, while amounts of the PSI and PSII components PsaB, PsaL,

Figure 5. Western Blot Analyses of Cotyledons and True Leaves in _L. japonicus._
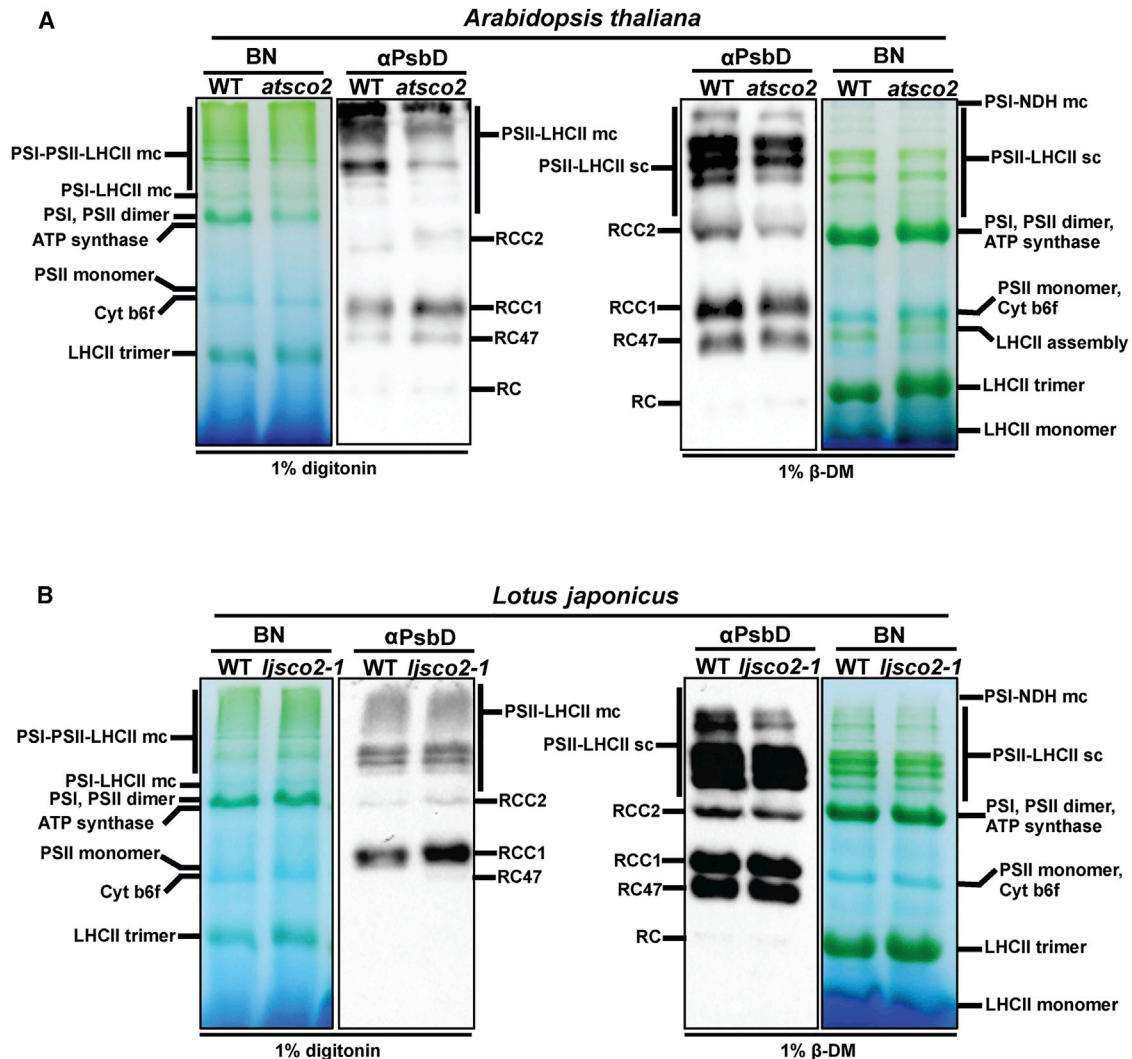The accumulation of proteins involved in protein quality control, photosynthesis and other processes was analyzed by western blotting of samples from 5-day-old cotyledons and 25-day-old true leaves of _Lotus_. Representative images of immunoblot analyses with the indicated antibodies are shown. Total protein extracts (10 μg of protein) from wild-type (WT) and the _ljsco2-1_ mutant were examined, together with a dilution series of the WT sample as indicated.

PsbD, and PsbC were lower than in WT, in agreement with previous reports for the _atsco2_ mutant. However, accumulation of PsbQ and PsbO was enhanced in variegated _ljsco2-1_ leaves. Both proteins form part of the oxygen-evolving complex and play a role in the supramolecular organization of PSII (Allahverdiyeva et al., 2013). Similarly, SUPPRESSOR OF VARIEGATION4 (SVR4) and its homolog SVR4L are both also overexpressed in variegated _ljsco2-1_ leaves. Interestingly, AtpB is clearly downregulated in both cotyledons and true leaves, whereas other chloroplastic proteins such as FNR and RbcL were slightly downregulated in the _ljsco2-1_ mutant while mitochondrial COXII and cytosolic ACT were virtually unchanged. In conclusion, absence of LjSCO2 causes mild responses in cotyledons but has more marked effects in true leaves.

SCO2 Is Involved in the Assembly or Repair of PSII Complexes

We next performed lpBN-PAGE (large-pore blue-native PAGE) on thylakoid samples isolated from true leaves of _Arabidopsis_ (Figure 6A) and _Lotus_ (Figure 6B), using as detergent either digitonin (left panels) or dodecyl-β-D-maltoside (β-DM, right panels). Digitonin facilitates the analysis of the labile PSI–LHCII megacomplexes, while β-DM permits efficient solubilization without disassembling PSII–LHCII supercomplexes (Jarvi et al.,

2011). To address the impact of lower levels of LHCB1 or PsbD (D2), we loaded samples containing equal amounts of chlorophyll to compensate for the quantitative differences in the latter between WT and _sco2_ mutants (Supplemental Figure 6B). After denaturation of the lpBN gels, immunoblot experiments using a specific antibody directed against the PsbD (D2) protein from the PSII reaction center permitted the detection of all PSII complexes (Figure 6A and 6B; Supplemental Figure 6C). In particular, when digitonin was used as detergent, a reduction in PSII–LHCII super- and megacomplexes, together with a general increase in the PSII assembly complexes RC, RC47, RCC1, and RCC2, was observed in _sco2_ mutants of both plant species. This suggests that the formation of super- and megacomplexes may be especially impaired in the absence of SCO2. Silver staining of the second-dimension gels corroborated that _sco2_ mutants in both species proportionally accumulate fewer high-molecular-weight complexes than smaller intermediate-sized complexes compared with WT plants (Supplemental Figure 7). In addition, an overaccumulation of LHCII trimers was noted in _sco2_ mutants, which is compatible with the involvement of SCO2 in the assembly of LHCs into the photosystems (Figure 6A and 6B). Because SCO2 was found in complexes compatible in size with PSI–LHCII and PSII–LHCII (Shimada et al., 2007), our results indicate that SCO2 has a role in the assembly or repair of PSII. To determine whether loss of SCO2 can affect state transitions, we determined the

Figure 6. SCO2 Is Required for PSII Supercomplex and Megacomplex Accumulation.
Thylakoid membranes from *Arabidopsis* **(A)** and *Lotus* **(B)** were solubilized in 1% digitonin (w/v) (left panels) or 1% β-DM (w/v) (right panels). Samples were fractionated by 5%–12% lpBN-PAGE as described in Methods. Subsequent denaturation and immunoblot analysis with a PsbD-specific antibody allows comparison of PSII complex pattern in wild-type (WT) and *sco2* mutants in both *Arabidopsis* and *Lotus*. The major protein complexes were assigned to individual bands as described by Jarvi et al. (2011). Supercomplexes (sc) and megacomplexes (mc) are indicated.
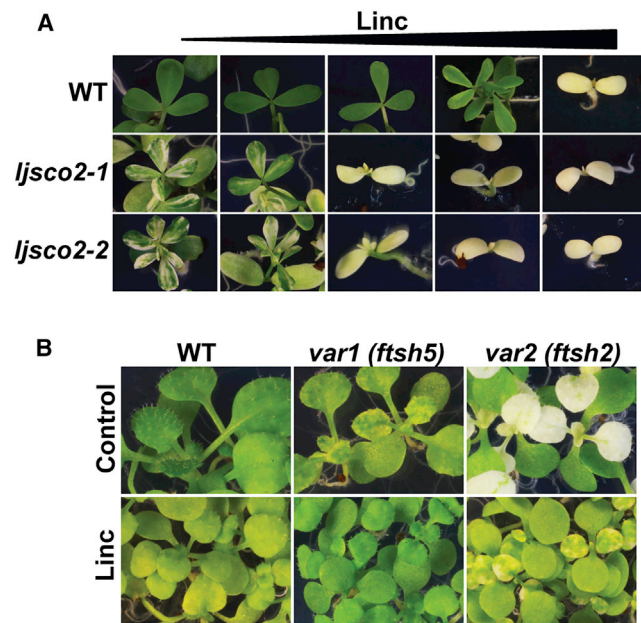
maximum fluorescence in state 2 (plants under red light) or state 1 (plants exposed to red and far-red light) (Bellafiore et al., 2005; Pribil et al., 2010). Although *ljsco2-1* mutant plants generally displayed lower chlorophyll fluorescence (according to the decrease in chlorophyll levels), they showed a WT-like response during the transition between state 2 and state 1 (Supplemental Figure 8). The degree of quenching of chlorophyll fluorescence can be quantified by calculating the parameter qT (Ruban and Johnson, 2009; Pribil et al., 2010). The qT values obtained for WT (0.083 ± 0.008) and *ljsco2-1* mutant (0.084 ± 0.008) plants were almost identical, indicating that in the absence of LjSCO2 the plants are still able to undergo reversible state transitions.

Inhibition of Protein Synthesis in the Chloroplast Does Not Suppress Variegation in *ljsco2* Mutants

The widely accepted threshold model for variegation postulates that an imbalance in the levels of chloroplast and nucleus-

encoded photosynthetic proteins is responsible for the impairments in chloroplast development (Liu et al., 2010b; Putarjunan et al., 2013). In line with this, the variegated phenotype of several mutants defective for nucleus-encoded proteins can be suppressed by mutations that reduce rates of protein synthesis in the chloroplast (Liu et al., 2010a, 2010c; Hu et al., 2015). Sublethal concentrations of chloroplast translation inhibitors are also able to suppress variegation (Yu et al., 2008). Therefore, we tested whether the chloroplast translation inhibitor lincomycin (Linc) suppresses variegation in *ljsco2* mutants. Surprisingly, none of the concentrations tested restored normal chloroplast development (Figure 7A and Supplemental Figure 9A). In fact, the *ljsco2* mutant is hypersensitive to Linc, unlike variegated *Arabidopsis* mutants such as *var1* (*ftsh5*) and *var2* (*ftsh2*) (Figure 7B) (Yu et al., 2008). Chloramphenicol, an alternative chloroplast translation inhibitor, was similarly unable to suppress leaf variegation in *ljsco2* mutants (Supplemental Figure 9B and 9C), implying that the molecular mechanism underlying *ljsco2*

Figure 7. Inhibition of Translation in the Chloroplast Does Not Suppress Variegation in *ljsco2* Mutants.

(A) Representative examples of *Lotus* wild-type (WT), and *ljsco2-1* and *ljsco2-2* mutant plants germinated and grown for 20 days on MS medium supplemented with increasing concentrations (from left to right: 0, 10, 50, 250, and 2500 μM) of lincomycin (Linc). None of the concentrations tested suppressed leaf variegation in the *ljsco2* mutants. On the contrary, the mutants proved to be abnormally sensitive to Linc-induced bleaching.

(B) Representative examples of *A. thaliana* WT, and *var1* (*ftsh5*) and *var2* (*ftsh2*) mutants grown in the presence or absence of 10 μM Linc. The variegation of true leaves in *ftsh* mutants is suppressed in the presence of Linc.

variegation might differ substantially from that responsible for other instances of variegation.

AtSCO2 Also Has a Role in Variegation in Photosynthetically Competent Leaves

The findings that *atsco2* leaves are smaller and paler than their WT counterparts under short-day conditions (Figure 2D) and that assembly of PSII complexes is impaired in the mutant (Figure 6A) demonstrate that the AtSCO2 function also extends beyond the cotyledon stage in *Arabidopsis*. The enhanced sensitivity of *ljsco2* mutants to Linc suggests a link between SCO2 and protein synthesis in the chloroplast. Therefore, a double mutant was generated in *Arabidopsis* by crossing *atsco2* with the *atclpr1* mutant (also named *svr2*) (Supplemental Figure 10), which was previously shown to suppress the variegation phenotype of the *var2* (*ftsh2*) mutant (Yu et al., 2008). In fact, *atclpr1* is impaired in chloroplast rRNA processing, a feature shared by several suppressors of variegation (Yu et al., 2008). As a consequence, chloroplast translation is inhibited in *atclpr1* and several representative plastid genes display normal levels of transcripts but reduced protein accumulation (Koussevitzky et al., 2007). Strikingly, the double mutant *atsco2 atclpr1* exhibited very pale and variegated true leaves (Figure 8A), which supports a function for AtSCO2 in photosynthetically competent leaves in *Arabidopsis*. The additive phenotype in the double mutant already becomes manifest at the seedling stage

(Figure 8B). This is in striking contrast to the variegated mutants *var2* (Yu et al., 2008) and *thf1* (Ma et al., 2015), which display reduced leaf variegation when the corresponding mutations are introduced into a background where protein synthesis in chloroplasts is compromised. Taken together, these results indicate a distinct mechanism of action for SCO2.
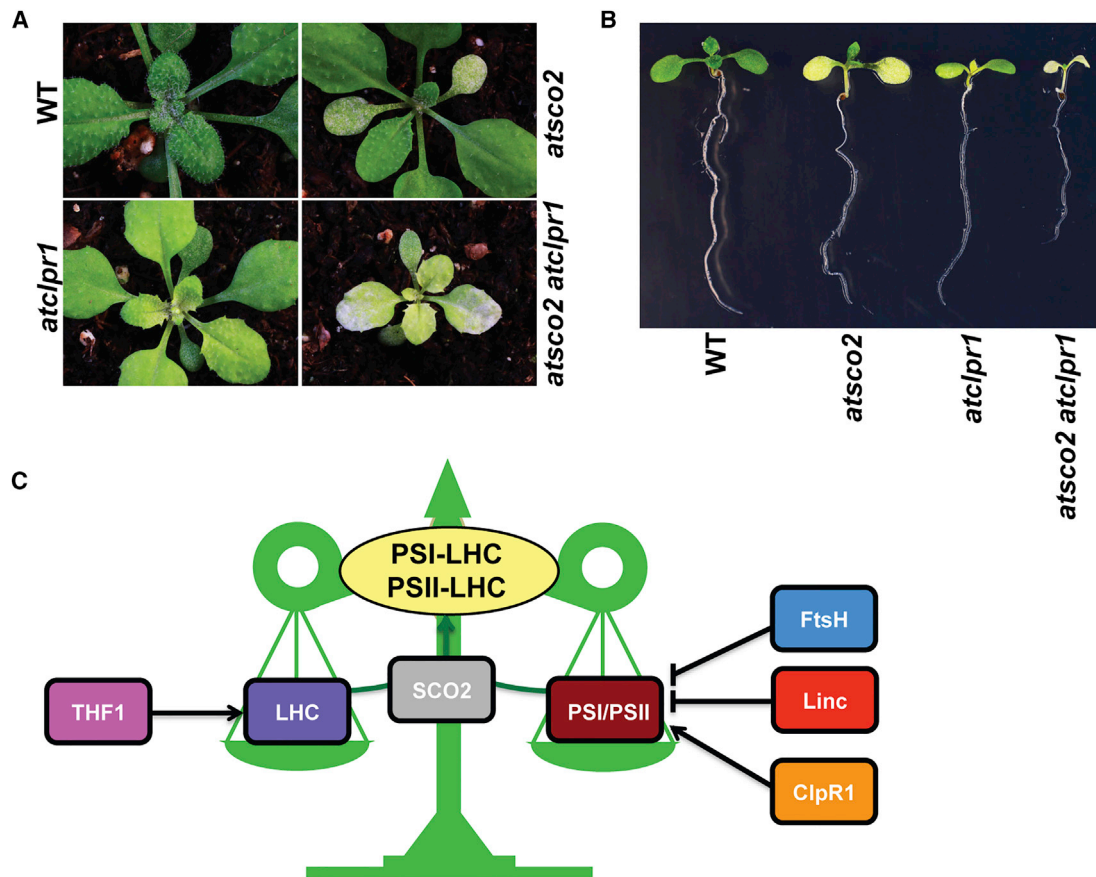
DISCUSSION

SCO2 Is a Conserved DNAJ-like Protein Involved in Chloroplast Biogenesis in Cotyledons and True Leaves

Chloroplast biogenesis in cotyledons and leaves are analogous processes, but there are some marked differences between them (Stoynova-Bakalova et al., 2004). A wide variety of mutants has been shown to affect leaf development, which requires cell division at the meristems, while cotyledons are formed during embryogenesis. Indeed, relatively few mutants display impaired chloroplast biogenesis specifically in cotyledons. In particular, mutants for SNOWY COTYLEDON2 (AtSCO2) with albino cotyledons but normal green true leaves have been found in two independent screens in *Arabidopsis* (Shimada et al., 2007; Albrecht et al., 2008). Therefore, AtSCO2 was assumed to be a cotyledon-specific factor required for normal accumulation of the photosynthetic machinery. However, in this study we report three independent mutant lines for *L. japonicus* SCO2, all of which display pale cotyledons and variegated true leaves (Figure 1 and Supplemental Figure 1). SCO2 belongs to the DNAJ-like family but forms a distinct clade in plants, suggesting that the protein has a conserved and specific function (Supplemental Figure 2). Indeed, mutants for the closest paralog of AtSCO2 do not exhibit albino cotyledons or defects in chloroplast biogenesis (Lu et al., 2011). Furthermore, we observed that *ljsco2* mutants are also affected during the transition from dark (etioplast) to light (chloroplast) and in the accumulation of PSI (Figure 2A). Surprisingly, we also found that true leaves are clearly affected in *atsco2* mutants grown under short-day conditions, a phenotype not reported previously (Figure 2D). This finding reveals a new role in leaf development for SCO2, and indicates that it has a wider significance than initially suspected.

SCO2 Is Required for the Assembly or Repair of LHC in the Photosystems

Chaperones and proteases act coordinately as constituents of the protein quality control system that is essential for plant survival (Lee et al., 2009; Pulido et al., 2016). In chloroplasts, it is well known that the chaperone Hsp70 post-translationally regulates PSII assembly and repair, and contributes to the heat-shock response and protein import into the chloroplast (Schroda et al., 1999; Su and Li, 2008, 2010; Shi and Theg, 2010). The specificity of Hsp70 is known to be determined by its DNAJ-like partners, which act as adaptors that recognize unfolded substrates and transfer them to the chaperone for refolding. In classical A-type DNAJ proteins, the J domain is responsible for the interaction with Hsp70, while the zinc finger interacts with the substrate (Miernyk, 2001; Rajan and D'Silva, 2009; Kampinga and Craig, 2010). In the absence of a conserved J domain, DNAJ-like proteins are assumed to exhibit a chaperone-like activity independently of Hsp70, interacting with and stabilizing client substrates, such as the ORANGE (OR) proteins required for accumulation of phytoene synthase

Figure 8. A Proposed Model Illustrating How SCO2 Functions in the Assembly or Repair of Photosynthetic Complexes and Has a Role in Leaf Variegation.

Representative 3-week-old *Arabidopsis* plants **(A)** and 10-day-old seedlings **(B)** grown under long-day conditions. Genotypes: WT, *atsco2*, *atclpr1*, and *atsco2 atclpr1*. In the proposed model **(C)**, THF1 and FtsH affect the accumulation of LHC (PSI and PSII) and the reaction center protein D1 (PSII), respectively. In both cases the balance required for the assembly of photosynthetic complexes is disrupted, hence producing variegation. Decreasing protein biosynthesis in the chloroplast (absence of ClpR1 or applying Linc) reduces the levels of several chloroplast-encoded photosynthetic proteins, partially restoring the proper ratio for complex assembly and suppressing variegation. However, SCO2 acts in a later step of the pathway, assisting in the assembly or repair of LHC with PSI and PSII. Therefore, the role of SCO2 in inhibition of leaf variegation cannot be suppressed by downregulation of protein biosynthesis in the chloroplast.

(PSY) and the biosynthesis of carotenoids (Zhou et al., 2015). Interestingly, SCO2's closest homolog, LOW QUANTUM YIELD OF PHOTOSYSTEM II 1 (LQY1), shows disulfide isomerase activity and interacts with the PSII core complex (Lu et al., 2011). Indeed, AtSCO2 itself reduces cysteines in artificial substrates *in vitro* (Shimada et al., 2007; Muranaka et al., 2012). Both LQY1 and AtSCO2 participate in the assembly or repair of PSII complexes, but differ in the number of pairs of cysteines conserved (only two in SCO2, Supplemental Figure 2), and in their interaction partners, as revealed by BN-PAGE analyses (Shimada et al., 2007; Lu et al., 2011). LQY1 was found to comigrate with the PSII core monomer (RCC1) and the CP43-less PSII monomer (RC47) after exposure to high light levels, which suggests a role in repair and reassembly of PSII complexes (Lu et al., 2011). AtSCO2 associates with PSI–LHCII and PSII–LHCII complexes, but further experiments are required to characterize these complexes.

We have demonstrated that *sco2* mutants in both *Arabidopsis* and *Lotus* not only accumulate reduced amounts of PSII components but are defective in the biogenesis or repair of the PSII complexes in true leaves (Figure 6; Supplemental Figures 6C and 7). Thus, there is a general overaccumulation of the intermediate complexes RC, RC47, RCC1, and RCC2, with a concomitant build-up of LHCII trimers in *sco2* mutants. Accordingly, maximum quantum yield and electron transport rate of PSII are both reduced in *ljsco2* mutants (Figure 4A). However, PSI accumulation is also affected, as can be deduced from 77-K fluorescence emission experiments (Figure 2A) and previous reports (Figure 5) (Shimada et al., 2007; Albrecht et al., 2008). In addition, the levels of the ATP synthase subunit AtpB are decreased in the absence of LjSCO2 (Figure 5) such that other roles of LjSCO2 in thylakoid biogenesis and functioning, in addition to photosystem-related processes, cannot be ruled out. Although the only substrate known to interact with AtSCO2 *in vivo* is LHCB1 (Tanz et al., 2012), other putative targets have been proposed. Thus, analysis with the split-ubiquitin system has suggested the interaction of AtSCO2 with PSI (A1 and A2 subunits), as well as PSII (CP43 and CP47 subunits) (Muranaka et al., 2012). However, the *in vivo* relevance of these interactions remains to be studied. The effects on NPQ noted in *sco2* mutants might result from these complex interactions.

The *Lotus ljsco2-1* mutant displays a rapid increase in NPQ values upon illumination, but the values remain below the WT average until the situation is reversed in the relaxation phase (Figure 4B). Faster NPQ induction may be linked to pre-accumulation of zeaxanthin in the *ljsco2-1* mutant (Figure 4C), which is only detected in WT plants under high-light conditions (Supplemental Figure 5). Given that AtSCO2 interacts with LHCB1, it is not surprising that LjSCO2 has a role in the regulation of NPQ. LHCII is involved in thermal dissipation of the excess light energy absorbed during photosynthesis (Niyogi and Truong, 2013), and the downregulation of LHCB1 produces a decrease in NPQ values (Pietrzykowska et al., 2014). Interestingly, WT plants also show an increase in NPQ at higher temperatures (Bilger and Bjorkman, 1991) and after heat shock (Marutani et al., 2014). Moreover, paraquat treatment causes NPQ to peak at the beginning of the quenching phase (Moustaka et al., 2015), as in the *ljsco2-1* mutant. Therefore, perhaps other stress situations can also induce zeaxanthin levels. The fact that the *ljsco2-1* mutant is under constitutive stress, as indicated by the accumulation of zeaxanthin and tocopherols (Figure 4C and Supplemental Figure 5) and the higher levels of chaperones and proteases (Figure 5), might contribute to the observed alterations in NPQ.

SCO2 Constitutes a Novel Factor Involved in Leaf Variegation

Multiple factors have been reported to control leaf variegation. In *Arabidopsis*, *immutans* (*im*) and *variegated 2* (*var2*) mutants, which are defective in plastid terminal oxidase (PTOX) and the thylakoid protease FtsH2, respectively, are the best characterized chloroplast biogenesis mutants (Aluru et al., 2006; Foudree et al., 2012; Putarjunan et al., 2013). Loss of PTOX impairs the activity of phytoene desaturase, an enzyme in the carotenoid biosynthesis pathway (Ruiz-Sola and Rodriguez-Concepcion, 2012). PTOX is a central regulator of thylakoid redox and PSII excitation pressure, modulating the redox state of the PQ pool. Thus, the variegation seen in the absence of PTOX has been attributed to a redox imbalance in *Arabidopsis* (Rosso et al., 2009). Mutational inactivation of *PROTON GRADIENT REGULATION 5* (PGR5) or *CHLORORESPIRATORY REDUCTION 2* (CRR2) suppresses variegation in *im* mutants by reducing the excitation pressure (Munekage et al., 2002; Hashimoto et al., 2003; Okegawa et al., 2010). The suppression of variegation in *var2* mutants has uncovered a link with protein biosynthesis in the chloroplast. Several mutations affecting chloroplast translation or chloroplast RNA processing have been reported to suppress variegation in plants lacking FtsH2 (Park and Rodermel, 2004; Miura et al., 2007; Yu et al., 2008, 2011; Liu et al., 2010a). Furthermore, the variegated phenotype of a mutant named *thylakoid formation 1* (*thf1*) is also suppressed when chloroplast protein biosynthesis is impaired (Hu et al., 2015; Ma et al., 2015). Interestingly, THF1, like AtSCO2, interacts with LHCB1. However, the inhibition of chloroplast translation (Figure 7 and Supplemental Figure 9) does not suppress the variegation in *ljsco2*. Furthermore, the clearly additive effect seen in variegated true leaves in *atsco2 atclpr1* plants demonstrates that reducing rates of protein biosynthesis in the chloroplast actually exacerbates the defect in chloroplast biogenesis observed in the absence of SCO2 alone. Hence, we suggest that variegation in *ljsco2* mutants is controlled by a distinct molecular mechanism. In the model we propose

(Figure 8C), THF1 and FtsH affect the accumulation of LHCs and the PSII reaction center protein D1, respectively. In both cases the balance required for the assembly of photosynthetic megacomplexes is disrupted, hence producing variegation. Decreasing protein biosynthesis in the chloroplast (by deleting ClpR1 or applying inhibitors of chloroplast translation such as Linc) reduces the levels of chloroplast-encoded components of the photosynthetic machinery, partially restoring the stoichiometry required for complex assembly and suppressing variegation. However, the absence of SCO2 impaired the attachment of LHCs to PSI and PSII. In this genetic situation, the reduction of chloroplast translation with inhibitors or the introduction of the *atclpr1* mutation further aggravates the perturbation in the assembly of the photosystems with the antenna complexes (Figure 8C).

METHODS

Plant Material, Propagation, and Growth Conditions

Lotus japonicus sco2 mutants in the Gifu genetic background originate from the *LORE1* endogenous retrotransposon mutant population (www.lotus.au.dk) (Malolepszy et al., 2016). Three independent lines with a similar variegated phenotype identified as *ljsco2-1* (30096086), *ljsco2-2* (30099994), and *ljsco2-3* (30006602) were found to disrupt the coding region of the *LjSCO2* gene (*Lj3g3v0537380.1*). The ecotype Gifu B-129 served as the WT control. *Lotus* seeds were surface sterilized (Handberg and Stougaard, 1992) and grown on soil or solid Murashige and Skoog (MS) medium. For greening experiments, plants were exposed to light (100 µmol photons m^{-2} s^{-1}) for 4 h, then incubated in the dark at 22°C for 8 days. Pigments were extracted from whole seedlings immediately, and after 1 and 8 days of growth under long-day conditions (100 µmol photons m^{-2} s^{-1}).

The *A. thaliana sco2* mutant (NASC: N68145) in the Landsberg *erecta* background was initially isolated in an ethyl methanesulfonate screen for plants with pale cotyledons and green true leaves (Albrecht et al., 2008). The *atclpr1* mutant (SALK_088407) in the Columbia-0 background has been described previously (Koussevitzky et al., 2007; Pulido et al., 2016). After stratification for 3 days at 4°C, WT and mutant plants were grown on soil or MS agar plates with 1% sucrose.

Both *Arabidopsis* and *Lotus* plants were grown under controlled conditions in growth chambers at 22°C in long-day (16 h light/8 h dark, 100 µmol photons m^{-2} s^{-1}), short-day (8 h light/16 h dark, 100 µmol photons m^{-2} s^{-1}), continuous light (100 µmol photons m^{-2} s^{-1}), or high light (16 h light/8 h dark, 400 µmol photons m^{-2} s^{-1}).

When specified, *Arabidopsis* and *Lotus* were grown on plates supplemented with the indicated concentrations of chloramphenicol or Linc.

Nucleic Acid Analysis

Arabidopsis genomic DNA was isolated by a phenol- and chloroform-free method (Edwards et al., 1991). The *atclpr1* T-DNA insertion-junction sites were recovered by PCR using combinations of insertion- and gene-specific primers (Supplemental Table 1) and then sequenced. The whole *AtSCO2* gene was amplified and the band sequenced to detect the point mutation (Supplemental Figure 10).

L. japonicus DNA extraction and library preparation was performed as described earlier, and the sequencing output was analyzed using FSTpoolit v.0.33 software (Urbanski et al., 2012).

Total RNA was isolated from seedlings and leaf samples frozen in liquid nitrogen using TRIzol reagent (Invitrogen) according to the manufacturer's protocol. For each RNA sample, a pool of at least three individual plants

was used. One microgram of RNA was primed with oligo(dT) and reverse transcribed into complementary DNA using Superscript III reverse transcriptase (Invitrogen). Relative levels of *LjSCO2* transcripts in WT cotyledons and true leaves (from 25-day-old WT and mutant *Lotus* plants) were determined by quantitative real-time PCR (for primer sequences see Supplemental Table S1), which was performed with iQ SYBR Green Supermix using an IQ5 multicolor real-time PCR detection system (Bio-Rad) following a standard thermal profile (95°C for 5 min, 40 cycles of 95°C for 10 s, 55°C for 30 s, and 72°C for 20 s). The relative level of each transcript was referred to the level of the corresponding *UBIQUITIN* transcript. Analysis of the threshold cycles (Ct) with the iQ5 software (Bio-Rad) was performed for determining relative expression.

Fluorescence Measurements

In vivo room temperature chlorophyll *a* fluorescence of leaves of 8-week-old *Lotus* plants was measured using a Dual-PAM 100 (Walz) as described previously (Pesaresi et al., 2009). After a minimum of 30 min of dark adaptation, the minimal fluorescence (F_0) was measured. To determine the maximum fluorescence (F_m), a pulse (0.8 s) of saturating white light (5000 μmol photon m^{-1} s^{-1}) was applied. The ratio ($F_m - F_0$)/F_m was calculated as F_v/F_m, the maximum quantum yield of PSII. The electron transport rate through PSII (ETR II) was monitored at increasing light intensities and plotted as a light-response curve.

For NPQ induction, plants were dark-adapted overnight and slow kinetics were determined by applying red actinic light (830 μmol photons m^{-2} s^{-1}) for 30 min, followed by a succession of white light pulses (8000 μmol photons m^{-2} s^{-1}, duration 600 ms) administered at 60-s intervals. NPQ was calculated as ($F_m - F_m'$)/F_m' and Φ_{II} as ($F_m - F_s$)/F_m.

False-color images representing F_v/F_m levels in WT and mutant leaves were produced using an Imaging PAM chlorophyll fluorometer equipped with the computer-operated PAM control unit IMAG-MAXI (Walz).

State transitions were measured by pulse-amplitude modulation fluorometry (PAM) as described previously (Pribil et al., 2010). Five plants of each genotype growing under long-day conditions were dark-adapted and analyzed using the Dual-PAM (Walz). Pulses of red light (5000 μmol photons m^{-2} s^{-1}, 0.5 s) were used to determine the maximum fluorescence. After illumination with red light (35 μmol photons m^{-2} s^{-1}, 15 min), state 1 was induced by adding far-red light (maximal light intensity corresponding to level 20 in the Dual-PAM setting, 15 min) and F_M1 was determined. Next, state 2 was induced by switching off the far-red light (only red light, 15 min) and F_M2 was measured. qT was calculated as ($F_M1 - F_M2$)/F_M1 (Ruban and Johnson, 2009).

Metabolite Analysis

Standard chlorophyll determinations were performed as described previously (Lichtenthaler and Wellburn, 1983). In brief, photosynthetic pigments were extracted by shaking 50-mg (fresh weight) samples of whole seedlings with 1 mL of 80% (v/v) ice-cold acetone in the dark at 4°C for 30 min. After centrifugation (10 000 × *g*, 2 min, 4°C), A_{663}, A_{647}, and A_{470} were recorded with a spectrophotometer (Ultrospec 3100, Amersham Biosciences) and pigment levels were calculated according to the following equation: chlorophyll $a = 12.25 A_{663} - 2.79 A_{647}$; chlorophyll $b = 21.50 A_{647} - 5.10 A_{663}$; chlorophyll total $= 7.15 A_{663} + 18.71 A_{647}$; carotenoids $= (1000 A_{470} - 1.82 \text{Chl}_a - 85.02 \text{Chl}_b)/198$.

Alternatively, HPLC analysis of chlorophylls, carotenoids, and tocopherols was performed as described by Rodriguez-Concepcion et al. (2004) using 4 μg of lyophilized 45-day-old *Lotus* samples and an Agilent 1200 series HPLC system (Agilent Technologies, http://www.agilent.com). Canthaxanthin was used as an internal standard for normalization, and appropriate carotenoid and tocopherol standards were used for quantification.

Computational Analysis

For sequence comparisons, orthologs of AtSCO2 (AT3G19220) were identified by BLAST. Sequences were aligned with MUSCLE (www.ebi.ac.uk/Tools/msa/muscle), and a phylogenetic tree rooted at midpoint was constructed using the neighbor-joining method in MEGA6 (megasoftware.net). The evolutionary distances were computed using the Poisson correction method, and the bootstrap test was performed with 2000 replications. Data used to create Supplemental Figure 2 can be retrieved under the following accession numbers: *A. thaliana* (AtSCO2, At3g19220; LQY1, AT1G75690; Tsip1, AT2G24860; BSD2, AT3G47650), *Brassica napus* (CDX92309), *Vitis vinifera* (XP_003631671), *Nicotiana sylvestris* (XP_009772536; XP_009761846), *Theobroma cacao* (XP_007042421) *Solanum tuberosum* (XP_006346429), *Populus trichocarpa* (XP_002313849), *L. japonicus* (Lj3g3v0537380), *Cucumis melo* (XP_008456126), *Cucumis sativus* (XP_004140700), *Solanum lycopersicum* (XP_010315236), *Malus domestica* (XP_017189504), *Glycine max* (NP_001242534; XP_003518841), *Zea mays* (NP_001144163), *Oryza sativa* (NP_001063376), *Hordeum vulgare* (BAJ85952), and *Phaseolus vulgaris* (XP_007156517).

Protein Isolation and Immunoblot Analyses

Protein analyses were performed as described by Pulido et al. (2013). In brief, total plant protein extracts were obtained from 50 mg of 25-day-old fresh tissue by grinding samples in liquid nitrogen. The powder was resuspended in 100 mL of ice-cold TKMES homogenization buffer (100 mM Tricine-KOH [pH 7.5], 10 mM KCl, 1 mM MgCl$_2$,1 mM EDTA, and 10% [w/v] sucrose) supplemented with 0.2% (v/v) Triton X-100, 1 mM DTT, and 20 mg/mL protease inhibitor cocktail (Sigma-Aldrich). The resuspended sample was centrifuged at 2300 *g* for 10 min at 4°C and the supernatant recovered for a second step of centrifugation. Supernatant protein concentration was determined using the Bio-Rad protein assay. After SDS–PAGE, the proteins were electrotransferred to Hybond-P polyvinylidene difluoride membranes (Amersham). After protein transfer was complete, membranes were incubated overnight at 4°C with the respective specific primary antibody (Agrisera) diluted 1:1000 for ClpC, LHCB1, PsaB, PsaL, PsbO, Cpn60, PsbQ, SVR4, SVR4L, and FNR; 1:5000 for AtpB, LHCB2, LHCB4, PsbD/D2, and PsbC; and 1:10 000 for RbcL and PsaA. Incubation with the horseradish peroxidase-conjugated secondary antibody (diluted 1:5000) was performed for 1 h at room temperature. Detection of immunoreactive bands was performed using the ECL Plus reagent (Amersham). Chemiluminescent signals were visualized using a ChemiDoc MP analyzer (Bio-Rad).

Thylakoid Isolation and SDS–PAGE

Four-week-old *A. thaliana* plants (grown under short-day conditions, 100–120 μmol photons m^{-2} s^{-1}, 22°C), or *L. japonicus* plants (grown under long-day conditions, 100–120 μmol photons m^{-2} s^{-1}, 22°C) were used. Thylakoids were isolated in the dark, following a previously described protocol (Jarvi et al., 2011). The grinding buffer contained 50 mM HEPES–KOH (pH 7.5), 330 mM sorbitol, 2 mM EDTA, 1 mM MgCl$_2$, 5 mM ascorbate, 0.05% BSA, and 10 mM sodium fluoride; shock buffer contained 50 mM HEPES–KOH (pH 7.5), 5 mM sorbitol, and 5 mM MgCl$_2$; and storage buffer contained 50 mM HEPES–KOH (pH 7.5), 100 mM sorbitol, and 10 mM MgCl$_2$. Total chlorophyll in the thylakoid fractions was determined after extraction with 80% acetone as described above. For SDS–PAGE, samples containing 0.5, 1, 2, and 3 μg of chlorophyll were resuspended in SDS–PAGE loading buffer supplemented with 200 mM DTT, and boiled at 95°C for 5 min. The samples were then centrifuged at 21 000 *g* for 2 min and loaded in SDS–PAGE gels.

Large-Pore Blue-Native PAGE (lpBN-PAGE)

From the thylakoid membranes, 12 μg of chlorophyll was incubated with 1% digitonin or 1% β-DM according to Jarvi et al. (2011) and the solubilized fraction was loaded on a native gradient gel (3.5%–12.5% [w/v], acrylamide/bisacrylamide ratio 32:1) topped with a 3% (w/v) stacking gel (ratio 1:4). After electrophoresis, the native gel was treated

for 1.5 h with Laemmli buffer (138 mM Tris–HCl [pH 6.8], 6 M urea, 22.2% [v/v] glycerol, 4.3% [w/v] SDS, and 200 mM DTT), and the separated protein complexes were transferred to a polyvinylidene fluoride membrane using the Turbo Transfer system (Bio-Rad).

Low-Temperature (77 K) Fluorescence Measurements

The accumulation of PSI and PSII was evaluated by using the low-temperature (77 K) fluorescence emission spectra of intact leaves frozen in liquid nitrogen. The fluorescence emission spectra were recorded *in vivo* from 600 to 800 nm using a spectrofluorometer (Photon Technology International, Lawrenceville, NJ) and an excitation wavelength of 435 nm. The peak level of the PSI fluorescence at 730 nm was compared with the fluorescence maximum of PSII at 680 nm.

SUPPLEMENTAL INFORMATION

Supplemental Information is available at *Molecular Plant Online*.

AUTHOR CONTRIBUTIONS

N.Z., D.L., and P.P. conceived and designed the experiments. N.Z., N.S., O.S.-I., J. Su, and P.P. performed the experiments. N.Z. N.S., M.P., J. Stougaard, M.R.-C., D.L., and P.P analyzed the data. D.L. and P.P. wrote the paper.

REFERENCES

Albrecht, V., Ingenfeld, A., and Apel, K. (2006). Characterization of the snowy cotyledon 1 mutant of *Arabidopsis thaliana*: the impact of chloroplast elongation factor G on chloroplast development and plant vitality. Plant Mol. Biol. **60**:507–518.

Albrecht, V., Ingenfeld, A., and Apel, K. (2008). Snowy cotyledon 2: the identification of a zinc finger domain protein essential for chloroplast development in cotyledons but not in true leaves. Plant Mol. Biol. **66**:599–608.

Albrecht, V., Simkova, K., Carrie, C., Delannoy, E., Giraud, E., Whelan, J., Small, I.D., Apel, K., Badger, M.R., and Pogson, B.J. (2010). The cytoskeleton and the peroxisomal-targeted snowy cotyledon3 protein are required for chloroplast development in *Arabidopsis*. Plant Cell **22**:3423–3438.

Allahverdiyeva, Y., Suorsa, M., Rossi, F., Pavesi, A., Kater, M.M., Antonacci, A., Tadini, L., Pribil, M., Schneider, A., Wanner, G., et al. (2013). *Arabidopsis* plants lacking PsbQ and PsbR subunits of the oxygen-evolving complex show altered PSII super-complex organization and short-term adaptive mechanisms. Plant J. **75**:671–684.

Aluru, M.R., Yu, F., Fu, A., and Rodermel, S. (2006). *Arabidopsis* variegation mutants: new insights into chloroplast biogenesis. J. Exp. Bot. **57**:1871–1881.

Bellafiore, S., Barneche, F., Peltier, G., and Rochaix, J.D. (2005). State transitions and light adaptation require chloroplast thylakoid protein kinase STN7. Nature **433**:892–895.

Bilger, W., and Bjorkman, O. (1991). Temperature dependence of violaxanthin de-epoxidation and non-photochemical fluorescence quenching in intact leaves of *Gossypium hirsutum* L. and *Malva parviltora* L. Planta **184**:226–234.

Edwards, K., Johnstone, C., and Thompson, C. (1991). A simple and rapid method for the preparation of plant genomic DNA for PCR analysis. Nucleic Acids Res. **19**:1349.

Foudree, A., Putarjunan, A., Kambakam, S., Nolan, T., Fussell, J., Pogorelko, G., and Rodermel, S. (2012). The mechanism of variegation in immutans provides insight into chloroplast biogenesis. Front Plant Sci. **3**:260.

Fristedt, R., Williams-Carrier, R., Merchant, S.S., and Barkan, A. (2014). A thylakoid membrane protein harboring a DnaJ-type zinc finger domain is required for photosystem I accumulation in plants. J. Biol. Chem. **289**:30657–30667.

Fukai, E., Soyano, T., Umehara, Y., Nakayama, S., Hirakawa, H., Tabata, S., Sato, S., and Hayashi, M. (2012). Establishment of a *Lotus japonicus* gene tagging population using the exon-targeting endogenous retrotransposon LORE1. Plant J. **69**:720–730.

Handberg, K., and Stougaard, J. (1992). *Lotus japonicus*, an autogamous, diploid legume species for classical and molecular genetics. Plant J. **2**:487–496.

Hashimoto, M., Endo, T., Peltier, G., Tasaka, M., and Shikanai, T. (2003). A nucleus-encoded factor, CRR2, is essential for the expression of chloroplast ndhB in *Arabidopsis*. Plant J. **36**:541–549.

Hu, F., Zhu, Y., Wu, W., Xie, Y., and Huang, J. (2015). Leaf variegation of thylakoid formation1 is suppressed by mutations of specific sigma-factors in *Arabidopsis*. Plant Physiol. **168**:1066–1075.

Jarvi, S., Suorsa, M., Paakkarinen, V., and Aro, E.M. (2011). Optimized native gel systems for separation of thylakoid protein complexes: novel super- and mega-complexes. Biochem. J. **439**:207–214.

Jarvis, P., and Lopez-Juez, E. (2013). Biogenesis and homeostasis of chloroplasts and other plastids. Nat. Rev. Mol. Cell Biol. **14**:787–802.

Kampinga, H.H., and Craig, E.A. (2010). The HSP70 chaperone machinery: J proteins as drivers of functional specificity. Nat. Rev. Mol. Cell Biol. **11**:579–592.

Kleine, T., and Leister, D. (2016). Retrograde signaling: organelles go networking. Biochim. Biophys. Acta **1857**:1313–1325.

Koussevitzky, S., Stanne, T.M., Peto, C.A., Giap, T., Sjogren, L.L., Zhao, Y., Clarke, A.K., and Chory, J. (2007). An *Arabidopsis thaliana* virescent mutant reveals a role for ClpR1 in plastid development. Plant Mol. Biol. **63**:85–96.

Lee, S., Lee, D.W., Lee, Y., Mayer, U., Stierhof, Y.D., Lee, S., Jurgens, G., and Hwang, I. (2009). Heat shock protein cognate 70-4 and an E3 ubiquitin ligase, CHIP, mediate plastid-destined precursor degradation through the ubiquitin-26S proteasome system in *Arabidopsis*. Plant Cell **21**:3984–4001.

Lichtenthaler, H.K., and Wellburn, A.R. (1983). Determination of total carotenoids and chlorophylls a and b of leaf extracts in different solvents. Biochem. Soc. Trans. **603**:591–592.

Liu, X., Rodermel, S.R., and Yu, F. (2010a). A var2 leaf variegation suppressor locus, SUPPRESSOR OF VARIEGATION3, encodes a putative chloroplast translation elongation factor that is important for chloroplast development in the cold. BMC Plant Biol. **10**:287.

Liu, X., Yu, F., and Rodermel, S. (2010b). *Arabidopsis* chloroplast FtsH, var2 and suppressors of var2 leaf variegation: a review. J. Integr. Plant Biol. **52**:750–761.

Liu, X., Yu, F., and Rodermel, S. (2010c). An *Arabidopsis* pentatricopeptide repeat protein, SUPPRESSOR OF VARIEGATION7, is required for FtsH-mediated chloroplast biogenesis. Plant Physiol. **154**:1588–1601.

Lopez-Juez, E., and Pyke, K.A. (2005). Plastids unleashed: their development and their integration in plant development. Int. J. Dev. Biol. **49**:557–577.

Lu, Y., Hall, D.A., and Last, R.L. (2011). A small zinc finger thylakoid protein plays a role in maintenance of photosystem II in *Arabidopsis thaliana*. Plant Cell **23**:1861–1875.

Ma, Z., Wu, W., Huang, W., and Huang, J. (2015). Down-regulation of specific plastid ribosomal proteins suppresses thf1 leaf variegation, implying a role of THF1 in plastid gene expression. Photosynth. Res. **126**:301–310.

Malolepszy, A., Mun, T., Sandal, N., Gupta, V., Dubin, M., Urbanski, D.F., Shah, N., Bachmann, A., Fukai, E., Hirakawa, H., et al. (2016). The LORE1 insertion mutant resource. Plant J. **88**:306–317.

Marutani, Y., Yamauchi, Y., Miyoshi, A., Inoue, K., Ikeda, K., Mizutani, M., and Sugimoto, Y. (2014). Regulation of photochemical energy transfer accompanied by structural changes in thylakoid membranes of heat-stressed wheat. Int. J. Mol. Sci. **15**:23042–23058.

Miernyk, J.A. (2001). The J-domain proteins of *Arabidopsis thaliana*: an unexpectedly large and diverse family of chaperones. Cell Stress Chaperones **6**:209–218.

Miura, E., Kato, Y., Matsushima, R., Albrecht, V., Laalami, S., and Sakamoto, W. (2007). The balance between protein synthesis and degradation in chloroplasts determines leaf variegation in *Arabidopsis* yellow variegated mutants. Plant Cell **19**:1313–1328.

Moustaka, J., Tanou, G., Adamakis, I.D., Eleftheriou, E.P., and Moustakas, M. (2015). Leaf age-dependent photoprotective and antioxidative response mechanisms to paraquat-induced oxidative stress in *Arabidopsis thaliana*. Int. J. Mol. Sci. **16**:13989–14006.

Munekage, Y., Hojo, M., Meurer, J., Endo, T., Tasaka, M., and Shikanai, T. (2002). PGR5 is involved in cyclic electron flow around photosystem I and is essential for photoprotection in *Arabidopsis*. Cell **110**:361–371.

Muranaka, A., Watanabe, S., Sakamoto, A., and Shimada, H. (2012). *Arabidopsis* cotyledon chloroplast biogenesis factor CYO1 uses glutathione as an electron donor and interacts with PSI (A1 and A2) and PSII (CP43 and CP47) subunits. J. Plant Physiol. **169**:1212–1215.

Niyogi, K.K., and Truong, T.B. (2013). Evolution of flexible non-photochemical quenching mechanisms that regulate light harvesting in oxygenic photosynthesis. Curr. Opin. Plant Biol. **16**:307–314.

Okegawa, Y., Kobayashi, Y., and Shikanai, T. (2010). Physiological links among alternative electron transport pathways that reduce and oxidize plastoquinone in *Arabidopsis*. Plant J. **63**:458–468.

Park, S., and Rodermel, S.R. (2004). Mutations in ClpC2/Hsp100 suppress the requirement for FtsH in thylakoid membrane biogenesis. Proc. Natl. Acad. Sci. USA **101**:12765–12770.

Pesaresi, P., Hertle, A., Pribil, M., Kleine, T., Wagner, R., Strissel, H., Ihnatowicz, A., Bonardi, V., Scharfenberg, M., Schneider, A., et al. (2009). *Arabidopsis* STN7 kinase provides a link between short- and long-term photosynthetic acclimation. Plant Cell **21**:2402–2423.

Pietrzykowska, M., Suorsa, M., Semchonok, D.A., Tikkanen, M., Boekema, E.J., Aro, E.M., and Jansson, S. (2014). The light-harvesting chlorophyll a/b binding proteins Lhcb1 and Lhcb2 play complementary roles during state transitions in *Arabidopsis*. Plant Cell **26**:3646–3660.

Pribil, M., Pesaresi, P., Hertle, A., Barbato, R., and Leister, D. (2010). Role of plastid protein phosphatase TAP38 in LHCII dephosphorylation and thylakoid electron flow. PLoS Biol. **8**:e1000288.

Pulido, P., Toledo-Ortiz, G., Phillips, M.A., Wright, L.P., and Rodriguez-Concepcion, M. (2013). *Arabidopsis* J-protein J20 delivers the first enzyme of the plastidial isoprenoid pathway to protein quality control. Plant Cell **25**:4183–4194.

Pulido, P., Llamas, E., Llorente, B., Ventura, S., Wright, L.P., and Rodriguez-Concepcion, M. (2016). Specific Hsp100 chaperones determine the fate of the first enzyme of the plastidial isoprenoid pathway for either refolding or degradation by the stromal Clp protease in *Arabidopsis*. PLoS Genet. **12**:e1005824.

Putarjunan, A., Liu, X., Nolan, T., Yu, F., and Rodermel, S. (2013). Understanding chloroplast biogenesis using second-site suppressors of immutans and var2. Photosynth. Res. **116**:437–453.

Rajan, V.B., and D'Silva, P. (2009). *Arabidopsis thaliana* J-class heat shock proteins: cellular stress sensors. Funct. Integr. Genomics **9**:433–446.

Rodriguez-Concepcion, M., Fores, O., Martinez-Garcia, J.F., Gonzalez, V., Phillips, M.A., Ferrer, A., and Boronat, A. (2004). Distinct light-mediated pathways regulate the biosynthesis and exchange of isoprenoid precursors during *Arabidopsis* seedling development. Plant Cell **16**:144–156.

Rosso, D., Bode, R., Li, W., Krol, M., Saccon, D., Wang, S., Schillaci, L.A., Rodermel, S.R., Maxwell, D.P., and Huner, N.P. (2009). Photosynthetic redox imbalance governs leaf sectoring in the *Arabidopsis thaliana* variegation mutants immutans, spotty, var1, and var2. Plant Cell **21**:3473–3492.

Ruban, A.V., and Johnson, M.P. (2009). Dynamics of higher plant photosystem cross-section associated with state transitions. Photosynth. Res. **99**:173–183.

Ruckle, M.E., and Larkin, R.M. (2009). Plastid signals that affect photomorphogenesis in *Arabidopsis thaliana* are dependent on GENOMES UNCOUPLED 1 and cryptochrome 1. New Phytol. **182**:367–379.

Ruiz-Sola, M.A., and Rodriguez-Concepcion, M. (2012). Carotenoid biosynthesis in *Arabidopsis*: a colorful pathway. *Arabidopsis* Book **10**:e0158.

Sakamoto, W., Miyagishima, S.Y., and Jarvis, P. (2008). Chloroplast biogenesis: control of plastid development, protein import, division and inheritance. *Arabidopsis* Book **6**:e0110.

Schroda, M., Vallon, O., Wollman, F.A., and Beck, C.F. (1999). A chloroplast-targeted heat shock protein 70 (HSP70) contributes to the photoprotection and repair of photosystem II during and after photoinhibition. Plant Cell **11**:1165–1178.

Shi, L.X., and Theg, S.M. (2010). A stromal heat shock protein 70 system functions in protein import into chloroplasts in the moss *Physcomitrella patens*. Plant Cell **22**:205–220.

Shimada, H., Mochizuki, M., Ogura, K., Froehlich, J.E., Osteryoung, K.W., Shirano, Y., Shibata, D., Masuda, S., Mori, K., and Takamiya, K. (2007). *Arabidopsis* cotyledon-specific chloroplast biogenesis factor CYO1 is a protein disulfide isomerase. Plant Cell **19**:3157–3169.

Stoynova-Bakalova, E., Karanov, E., Petrov, P., and Hall, M.A. (2004). Cell division and cell expansion in cotyledons of *Arabidopsis* seedlings. New Phytol. **162**:471–479.

Su, P.H., and Li, H.M. (2008). *Arabidopsis* stromal 70-kD heat shock proteins are essential for plant development and important for thermotolerance of germinating seeds. Plant Physiol. **146**:1231–1241.

Su, P.H., and Li, H.M. (2010). Stromal Hsp70 is important for protein translocation into pea and *Arabidopsis* chloroplasts. Plant Cell **22**:1516–1531.

Tanz, S.K., Kilian, J., Johnsson, C., Apel, K., Small, I., Harter, K., Wanke, D., Pogson, B., and Albrecht, V. (2012). The SCO2 protein disulphide isomerase is required for thylakoid biogenesis and interacts with LHCB1 chlorophyll a/b binding proteins which affects chlorophyll biosynthesis in *Arabidopsis* seedlings. Plant J. **69**:743–754.

Urbanski, D.F., Malolepszy, A., Stougaard, J., and Andersen, S.U. (2012). Genome-wide LORE1 retrotransposon mutagenesis and high-throughput insertion detection in *Lotus japonicus*. Plant J. **69**:731–741.

Yu, F., Liu, X., Alsheikh, M., Park, S., and Rodermel, S. (2008). Mutations in SUPPRESSOR OF VARIEGATION1, a factor required for normal chloroplast translation, suppress var2-mediated leaf variegation in *Arabidopsis*. Plant Cell **20**:1786–1804.

Yu, F., Park, S.S., Liu, X., Foudree, A., Fu, A., Powikrowska, M., Khrouchtchova, A., Jensen, P.E., Kriger, J.N., Gray, G.R., et al. (2011). SUPPRESSOR OF VARIEGATION4, a new var2 suppressor locus, encodes a pioneer protein that is required for chloroplast biogenesis. Mol. Plant **4**:229–240.

Zhou, X., Welsch, R., Yang, Y., Alvarez, D., Riediger, M., Yuan, H., Fish, T., Liu, J., Thannhauser, T.W., and Li, L. (2015). *Arabidopsis* OR proteins are the major posttranscriptional regulators of phytoene synthase in controlling carotenoid biosynthesis. Proc. Natl. Acad. Sci. USA **112**:3558–3563.